Engineering Structures 133 (2017) 74–80

Contents lists available at ScienceDirect

Engineering Structures

journal homepage: www.elsevier.com/locate/engstruct

Energy harvesting from wind by a piezoelectric harvester

J.X. Tao [a], N.V. Viet [b], A. Carpinteri [c], Q. Wang [d,*]

[a] City University of Hong Kong Shenzhen Research Institute Building, Shenzhen Hi-Tech Industrial Park, Nanshan District, Shenzhen, China
[b] Department of Mechanical Engineering, Khalifa University, P.O. Box 127788, Abu Dhabi, United Arab Emirates
[c] Dept. of Structural, Geotechnical and Building Engineering, Politecnico di Torino, Corso Duca degli Abruzzi, Italy
[d] Department of Architecture and Civil Engineering, City University of Hong Kong, Kowloon, Hong Kong, China

ARTICLE INFO

Article history:
Received 3 November 2016
Accepted 10 December 2016
Available online 23 December 2016

Keywords:
Energy harvesting
Wind turbine
Piezoelectric harvester

ABSTRACT

A novel wind power harvester using piezoelectric effect is developed. This engineering structure device employs a wind turbine that extracts kinetic energy from the wind and converts it into the rotational motion of a shaft. The rotational shaft is connected to a Scotch yoke mechanism that is used for converting the rotational motion into linear vibrations of two piezoelectricity-levers through springs. A mathematic model is developed to calculate the root mean square value of the generated electric power. The influences of some practical considerations, such as the rotational speed of the wind turbine and the stiffness of the springs, on the root mean square of the generated power are discussed. The research results show that a power up to 150 W can be harvested for a piezoelectric wind turbine with a radius of blades of 1 m at the wind speed of 7.2 m/s, and the designed angular velocity of 50 rad/s.

1. Introduction

The increasingly consumption of traditional energies has caused serious energy crisis and environmental pollution on a global scale. Wind energy has been regarded as one of the most important renewable and green energy sources to solve the above problems [1]. Wind turbines have been used on one of the traditional ways of transferring kinetic energy from wind based on the principle of electromagnetic induction [2,3]. The power coefficient of the wind turbines with output of megawatt has been reported up to 40–45% at the optimal tip speed ratio of 5–7 [4]. However, these large-size turbine generators are always complex, costly, and normally induce a cogging torque which restricts the cut-in speed. For small wind turbines located in areas of unfavorable wind, they are of little practical use except in rare situations [5,6]. As a result, using unconventional approaches such as vortex induced vibration, galloping, flutter, and buffeting to harvest the wind energy have been recently proposed [7–15]. To provide a more efficient energy transfer process, piezoelectric technology is the most prominent candidate for converting mechanical energy to electricity with highest efficiencies and lowest costs owing to their high energy generation density, high voltage generation capability and simple configurations and economic benefits [16–18].

Early works about a piezoelectric windmill were carried in literatures [9,10]. The proposed devices had ten piezoelectric bimorphs arranged along the circumference of a horizontal-axis wind turbine rotor shaft in the cantilever beam form. The oscillating torque to vibrate the bimorphs was generated using the camshaft gear mechanism. A power of 7.5 mW at the wind speed of 10 mph was measured across a matching load of 6.7 kΩ. Authors also addressed some drawbacks of this device and gave an optimized structure made of only plastic parts in the later work [11]. Sirohi et al. [12] developed a piezoelectric energy harvesting device based on a galloping cantilever beam. The harvested wind energy is transferred to a galloping beam which has a rigid tip body with a D-shaped cross section. Piezoelectric sheets were bonded on the top and bottom surface of the beam. During galloping, vibrational motions are induced due to aerodynamic forces on the D-section, which is converted into electrical energy by the piezoelectric (PZT) sheets. Their experimental and analytical investigations of dynamic response and power output have shown that a maximum output power of 1.14 mW was measured at a wind velocity of 10.5 mph on a prototype device of length 235 mm and width 25 mm. Rezaei-Hosseinabadi et al.[13] presented a topology for piezoelectric energy harvesting made of a lift-based wind turbine and a piezoelectric beam with contactless vibration mechanism. The research results showed that a power density of 2 mW/cm^3 at 3.8 V at the wind speeds above 0.9 m/s can be achieved. Kishore et al. [14] designed an ultra-low start-up speed windmill made of a 72 mm diameter horizontal axis wind turbine rotor with 12 alter-

* Corresponding author.
E-mail address: quanwang@cityu.edu.hk (Q. Wang).

http://dx.doi.org/10.1016/j.engstruct.2016.12.021
0141-0296/

nating polarity magnets around its periphery and a 60 mm × 20 mm × 0.7 mm piezoelectric bimorph element having a magnet at its tip. This wind turbine was found to produce a peak electric power of 450 μW at the rated wind speed of 4.2 mph. Wu et al. [15] developed an effective and compact wind energy cantilever harvester subjected to a cross wind. Sufficient electrical energy output as high as 2 W was realized by tuning the resonant frequency of the harvester with a proof mass on the tip of the cantilever.

The aforementioned piezoelectric harvester devices have been mainly developed for energy supplies of wireless sensors. Therefore, most of them are small in sizes and the energy outputs are always in the scale of mW. Recent researches have shown that piezoelectric harvesters can harvest power range from several watts to hundreds of megawatts [19–23]. Xie et al. [19,22] developed a novel piezoelectric technology of energy harvesting from high-rise buildings and found that a power up to 432.2 MW can be realized. Viet et al. [23] proposed a floating energy harvester (FEH) using piezoelectric effect to harvest energy from water waves. Based on their simulated results, the root mean square (RMS) of 103 W can be achieved when the wave amplitude is 2 m. Hence, it is imperative to develop harvesters with high power using piezoelectric effect from wind.

In this research, a wind energy harvester using piezoelectric technique is developed. This proposed piezoelectric wind turbine incorporates the advantages of the conventional wind turbines and the piezoelectric harvesters. Wind turbine rotor blades with the shape optimized by aerodynamics and connected to a horizontal shaft are employed as the driving device. The wind-induced rotational motion of the shaft is converted into translation motion of a slotted rod through a Scotch yoke mechanism. Both sides of the slotted rod are linked with a spring used for transferring the linear motion into vibrations of two piezoelectricity-levers. The extracted wind power is directly converted into an applied force on the piezoelectric bars with levers for amplification to achieve a more efficient energy harvesting process. In addition, since only few structural components with small sizes are required, the current engineering structure device is much smaller and lighter than the conventional wind turbines.

2. Design and modeling methods

Design of a horizontal piezoelectric wind turbine is depicted in Fig. 1(a and b). Three blades with a radius of R are attached to a shaft that is used to link the internal piezoelectric device. As seen in Fig. 1(b), the main piezoelectric harvester consists of a Scotch yoke mechanism, two springs with stiffness coefficient of k_1, and two piezoelectric levers. The Scotch yoke, shown in Fig. 2, is a reciprocating motion mechanism, converting a rotational motion into a linear motion [24]. A slotted rod is used to make sure the motion is only in the direction perpendicular to the axis of the shaft by a cylindrical slider attached to a wheel. When the wheel rotates at an angular velocity, ω, the end points of the slotted rod are displaced from their initial position by an amount z_s (in time t) given by $z_s = Y\sin\omega t$, where Y is the amplitude, i.e. the distance between axles of the cylindrical slider and the shaft.

The piezoelectricity-lever device, shown in Fig. 3(a), consists of a lever with a long moment arm L_2 and a short moment arm L_1, a fixed-hinge for restricting linear displacements of the lever, and a piezoelectric bar with a Young's modulus, width, length, and height of E_P, a, b, and h, respectively. Since the piezoelectricity-lever devices are connected to the slotted rod by two springs, the harmonic motion is then converted into a spring force $F(t)$. The force location is at the point C and magnified n times at the point A on the piezoelectric bar by the lever mechanism, where n is the ratio of the length of the long moment arm to that of the short moment arm, $n = L_2/L_1$. Consequently, the electric power is generated by the piezoelectric-lever design.

In order to estimate the spring force $F(t)$, one of the piezoelectric lever is used as an example and is simplified as a damped single-degree-of-freedom (spring-mass) system, shown in Fig. 3(b) [23,25]. The equivalent mass m_e, spring stiffness k_e, and damping coefficient c can be derived from the material properties and dimensions of the lever and piezoelectric bar.

In the proposed design, the piezoelectric bar is firmly bonded on the lever at the region of point A. Due to the high tensile/compression stiffness of the piezoelectric bar in the force direction, the lever is supposed to be fixed throughout points A and B and equivalently transformed into a cantilever beam with a length of L_2. Hence, the equivalent mass m_e can be calculated as $m_e = \rho_l A_l L_1 n$, where ρ_l and A_l are material density and cross-section area, respectively. In this work, the lever is made of steel, and its cross-section is rectangular in shape with a width and height of s_1 and s_2, respectively. The dimensions of the lever face are selected as s_1 = 0.015 m and s_2 = 0.004 m, unless otherwise noted.

Since the applied force at point C induces an elastic deflection of the cantilever and axial deformation of the piezoelectric bar, the equivalent spring stiffness, k_e in Fig. 3(b) can be yielded as [26]:

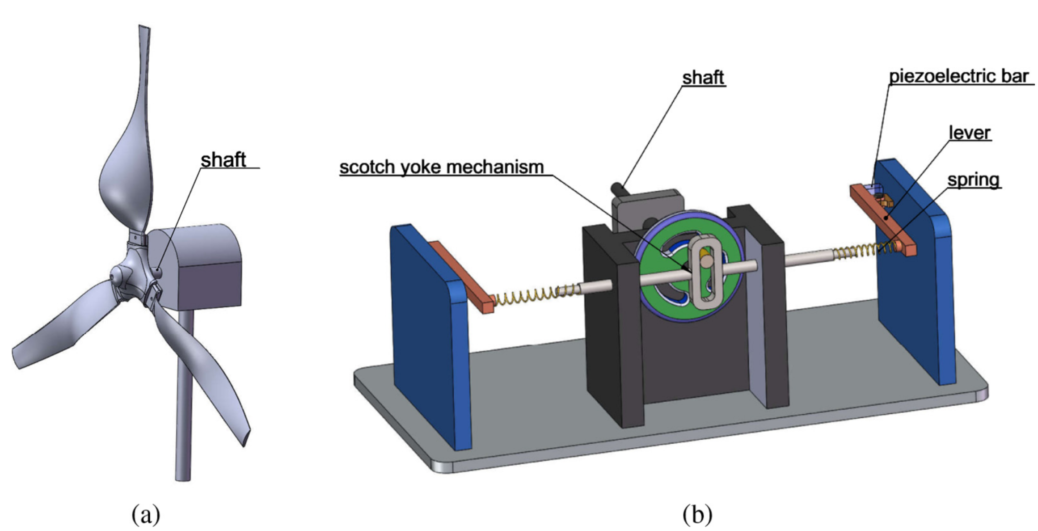

Fig. 1. Schematic diagram of a horizontal piezoelectric wind turbine: (a) an overview of the device, and (b) an internal structure of the device.

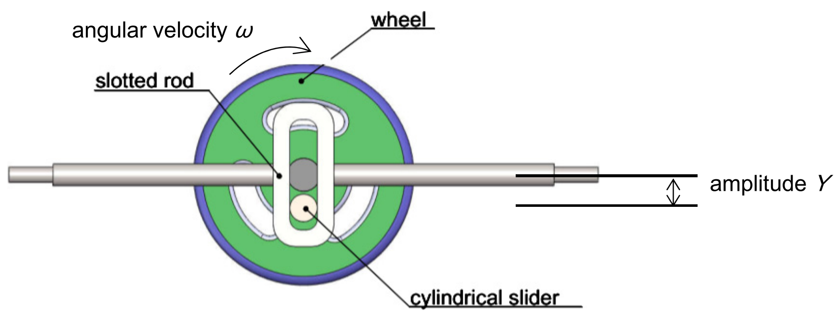

Fig. 2. Scotch yoke mechanism.

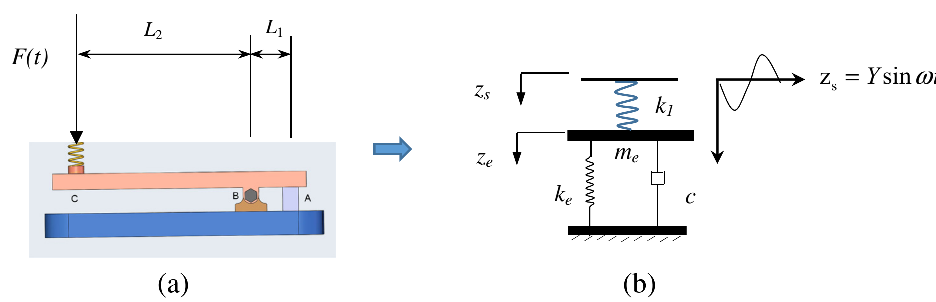

Fig. 3. Sketch of the piezoelectricity-lever device: (a) the lever in a realistic model, and (b) the equivalent mass-spring-damper model.

$$k_e = k_l k_p/(k_l + k_p), \quad k_l = E_l s_1 s_2^3/4(L_1 n)^3, \quad k_p = E_p ab/(n^2 h) \tag{1}$$

where k_l, E_l, k_p, E_p are spring constant and Young's modulus of the cantilever and piezoelectric bar, respectively.

The equivalent damping coefficient, shown in Fig. 3(b), can be expressed as a sum of the mechanical and electrical damping coefficients:

$$c = c_l + c_e \tag{2}$$

The mechanical damping force of the cantilever beam is triggered due to the internal structure damping force [27] and the friction between the viscous air and the cantilever beam in the vibration process, and hence is given as:

$$c_l = 2\xi\sqrt{k_l m_l} \tag{3}$$

where ξ is the damping ratio.

Besides the mechanical damping, there is an equivalent electric resistance when the work done by the spring force is converted into electricity [28]. The electrical damping coefficient, c_e, can be derived as [20]:

$$c_e = n^2 d_{33}^2 k_e^2/(\pi^2 c_a f) \tag{4}$$

where d_{33} is the piezoelectric constant in the polling direction; c_a is the electric capacity of the piezoelectric bar; f is the natural vibration frequency of the single-degree-of-freedom system.

Once the equivalent mass m_e, spring stiffness k_e, and damping coefficient c are obtained, we can get the equation of motion of the equivalent mass m_e using Newton's second law:

$$m_l\ddot{z}_e + c\dot{z}_e + k_e z_e = (z_s - z_e)k_1 \tag{5}$$

where z_s and z_e are the displacements of the slotted rod and the mass m_e, respectively. As is discussed above, horizontal motion of the slotted rod is expressed as $z_s = Y\sin\omega t$. Eq.(5) is then transformed as:

$$m_l\ddot{z}_e + c\dot{z}_e + (k_e + k_1)z_e = z_s k_1 = k_1 Y\sin\omega t \tag{6}$$

Hence, the model can be considered as a damped single-degree-of-freedom system subjected to an equivalent harmonic force:

$$m_l\ddot{z}_e + c\dot{z}_e + kz_e = F\sin\omega t \tag{7}$$

where $k = k_e + k_1$ and $F = k_1 Y$. We can easily obtain the displacement of equivalent mass m_e [29]:

$$z_e(t) = X\sin(\omega t - \phi) \tag{8}$$

where X is a constant that denotes the maximum amplitude of $z_e(t)$; ϕ is the phase angle:

$$X = \frac{F}{\sqrt{(k - m_l\omega^2)^2 + (c\omega)^2}}, \quad \tan\phi = \frac{c\omega}{k - m_l\omega^2} \tag{9}$$

Consequently, the relative displacement, $z(t)$, of the spring-mass system is:

$$z(t) = z_s(t) - z_e(t) \tag{10}$$

The magnified force, $F_m(t)$, applied to the piezoelectric bar can be computed by:

$$F_m(t) = n[k_1(z_s(t) - z_e(t)) - c\dot{z}_e(t)] \tag{11}$$

Hence the charge, voltage, and current generated by piezoelectric bar at time t can be expressed below:

$$Q(t) = d_{33}n[k_1 \cdot (z_s(t) - z_e(t)) - c\dot{z}_e(t)] \tag{12a}$$

$$V(t) = d_{33}n[k_1 \cdot (z_s(t) - z_e(t)) - c\dot{z}_e(t)]/c_a \tag{12b}$$

$$I(t) = d_{33}n[k_1 \cdot (\dot{z}_s(t) - \dot{z}_e(t)) - c\ddot{z}_e(t)] \tag{12c}$$

where the electric capacity of the piezoelectric material can be computed by [20]:

$$c_a = c_v \times a \times b \times 0.0001/(0.01 \times 0.01 \times l) \tag{13}$$

The generated electric power on each piezoelectric bar can be expressed below:

$$P_e(t) = I(t) \cdot V(t) \tag{14}$$

Since two piezoelectricity-lever devices are included in this device, the total generated electric power should be:

$$P_S(t) = 2P_e(t) \tag{15}$$

Finally, the expression of RMS of the electric power is provided. The RMS of the generated electric power from time 0 to t can be given as:

$$P_S^{rms} = 2\sqrt{\frac{1}{\tau}\int_0^{\tau} P_S^2 dt} \tag{16}$$

After the mathematic model is developed, we can estimate the generated charge and voltage from the piezoelectric bar as well as the RMS of the electric power. In this work, the material properties and dimensions of the piezoelectricity-lever device are provided in Table 1, unless otherwise noted. To find an efficient design of the piezoelectricity-lever and verify the effectiveness of the harvesting system, the aerodynamic model of wind turbine are adopted here. The mechanical power of the turbine, P, is given by [6]:

$$P = \frac{1}{2}\rho\pi R^2 v_W^3 C_P(\lambda) \tag{17}$$

where ρ is the air density, which equals 1.225 kg/m^3 at a temperature of 15 °C at sea level; R is the turbine radius; v_w is the wind speed. The factor $C_P(\lambda)$ is the power coefficient of the turbine, which is determined by the Tip-Speed Ratio λ . The tip-speed ratio λ is calculated as the ratio between the speed of the tip of a blade and the wind speed v_W:

$$\lambda = \frac{R\omega}{v_W} \tag{18}$$

The relation between the power coefficient C_P and the tip-speed ratio λ is determined by the shape of the blade. An empiric $C_P(\lambda)$ relations exist in literature [30] is used here:

$$C_P(\lambda) = 0.73\left(\frac{151}{\lambda} - 13.65\right)e^{\left(\frac{-18.4}{\lambda}+0.055\right)} \tag{19}$$

In the traditional horizontal-axis wind turbines, blades rotates only when the aerodynamic torque, T, exceeds the combined resistive torque of the drive train and generator, T_R. The starting rotating wind speed, when $T = T_R$, is called the cut-in speed. Wood [31] used the standard blade element theory to calculate the cut-in wind speed and provided the following equation:

$$U_C = \left(\frac{2T_R}{N\rho R^3 I_{cp}}\right)^{1/2} \tag{20}$$

where U_C is the cut-in speed; T_R is the resistive torque and can be expressed as $T_{Rmax} = k_1Y^2$ in this model; N is the number of blades;$\rho$is the air density; R is the blade tip radius; and I_{cp} is the chord-pitch integral determined by the shape of the blades.

From Eq. (20), we can find that the cut-in speed increases with the increasing resistive torque for the same blades. Therefore, for wind turbines located in areas of unfavorable wind, the resistive torque should be very small. In addition, increasing the number and the radius of the blades lead to a low cut-in speed for the same resistive torque.

3. Results and discussions

In this section, based on the above developed numerical model, we investigate the effectiveness of the piezoelectric wind turbine. Particularly, this work studies the effect of the spring stiffness, the amplitude, the angular velocity of the wind turbine, the ratio of moment arms, and the width (length) of the piezoelectric bar on the generated power. By using the aerodynamic model and empiric relations between the power coefficient C_P and the tip-speed ratio λ, the extracted mechanical power of a three-bladed wind turbine with radius of 1 m can be calculated, and the simulated results are compared with the RMS of the generated electric power.

The effect of spring stiffness k_1 and the amplitude Y on the RMS are first investigated because they determine the performance of the piezoelectric wind turbine. As mentioned before, for small wind turbine located in areas of unfavorable wind, the resistive torque of the electric generator should be very small. The field test results in the work of Clausen et al. [5] showed that for a designed two-bladed turbine with the radius of 2.5 m, the cut-in speed is less than 3 m/s when the resistive torque is 1 Nm. Wood [31] used a derived equation to calculate the cut-in speed and provided a value of 4.75 m/s for a three-bladed turbine with a length of 1 m. In this model, several small values ranging from 0.4 Nm to 1.2 Nm, of resistive torque, k_1Y^2, are used. Fig. 4 gives the effect of spring stiffness k_1, on the RMS of the generated electric power when the angular velocity, ratio of moment arms, and the width of the piezoelectric bar are 50 rad/s, 20, and 0.015 m, respectively. It is revealed from Fig. 4 that, when $k_1Y^2$is set as a constant, the RMS increases nonlinearly with a rise of the spring stiffness. When the stiffness changes from 5000 N/m to 40,000 N/m, the RMS increases from 15 W and 30 W to 60 W and 180 W corresponding to the resistive torque of 0.4 Nm and 1.2 Nm, respectively. This observation is interpreted by the fact that the force applied to the piezoelectric bar is proportional to k_1Y according to Eq. (11). When the resistive torque k_1Y^2 keeps a constant, a growth in the stiffness of springs will lead to a decline in the value of k_1Y, shown in Fig. 5, and correspondingly an enhancement in the force applied to the piezoelectric bar. The finding indicates that increasing the stiffness of the spring and decreasing the amplitude to keep a constant resistive torque can get a higher energy harvesting efficiency. In addition, increasing the amplitude Y and keeping a constant stiffness of the spring can also enhance the applied force k_1Y. But it should be noted here, the resistive torque will increase accordingly, which will make the turbine less effective at low speed wind regions.

The effect of the angular velocity of the wind turbine on the RMS is shown in Fig. 6. The stiffness of the spring, the amplitude, and the ratio of moment arms are set as 40,000 N/m, 0.005 m, and 20, respectively. It is seen clearly that the RMS increases nonlinearly from 0 W to 252 W with a rise in the angular velocity from 0 rad/s to 100 rad/s. This observation is mainly because that an increase in the angular velocity leads to a decrease in the period of the equivalent harmonic force, and hence causes an increase in the kinetic energy of the harvesting system and the generated electric power. Actually, the optimal angular velocity can be determined by Eqs. (17)–(19). In the real design, a large power coeffi-

Table 1
Material properties and dimensions of the piezoelectricity (PZT4)-lever device.

Piezoelectricity (PZT4)-lever device							
a (m)	b (m)	h (m)	l_1 (m)	ξ	d_{33} (C/N)	E_p (N/m^2)	E_l (N/m^2)
0.015–0.025	0.015–0.025	0.1	0.02	0.0017	3e−10	7.5e10	2.1e11

C_v(nF) 0.375 for the piezoelectric patch with the geometry of 0.01 m, 0.01 m, 0.0001 m.

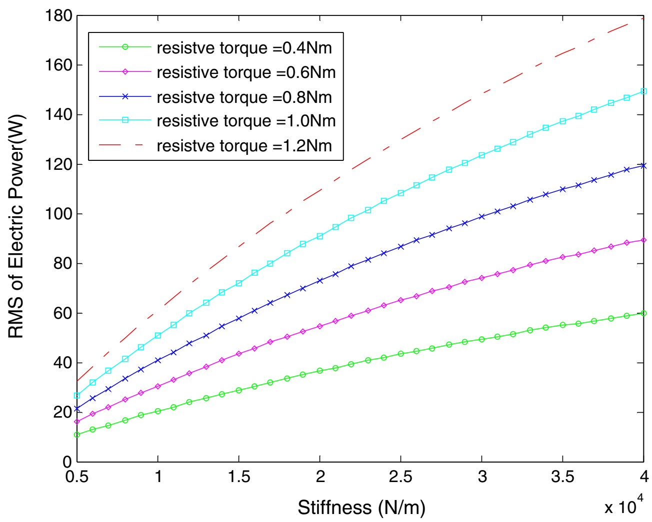

Fig. 4. RMS of the electric power versus stiffness of spring.

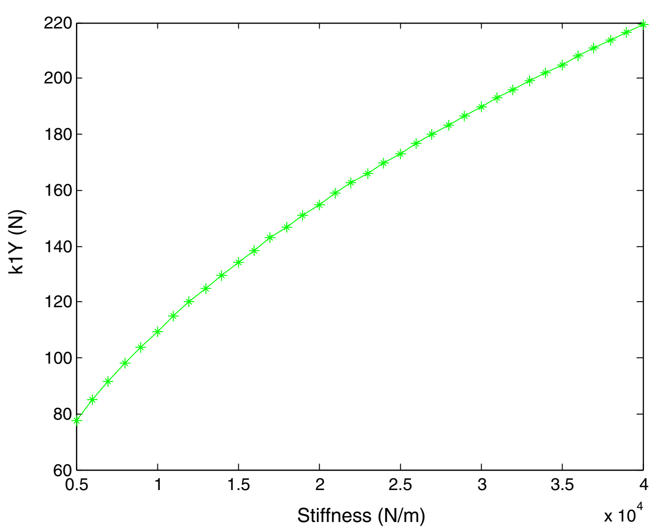

Fig. 5. The stiffness of the spring versus k_1Y.

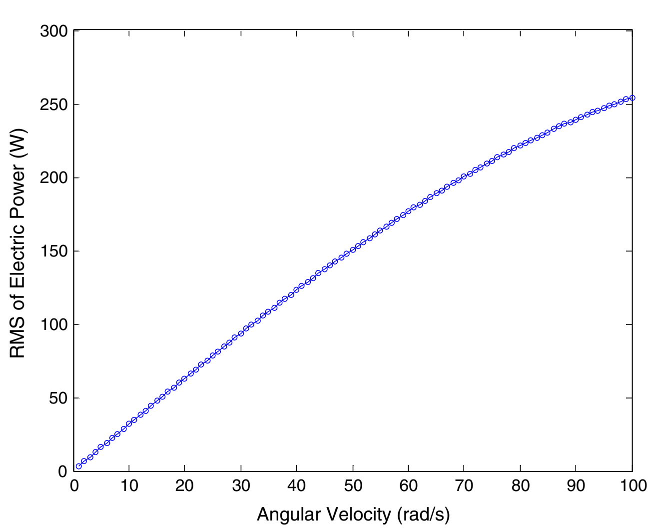

Fig. 6. RMS of the electric power versus the angular velocity.

cient C_P should be adopted in order to extract a high power from wind. The maximal value of C_P obtained from Eq. (19) is 0.44 for a tip-speed ratio λ of 6.91. Using the above values and substituting a designed wind speed into Eq. (17) and (18), we can calculate the extracted mechanical power P and the corresponding angular velocity ω.

As has been noted, wind turbine starts to rotate only when the wind speed is larger than the cut-in speed. For a given resistive torque, the cut-in speed can be estimated based on Eq. (20). Using the chord-pitch integral in Ref. [31], the calculated cut-in speed for a three-bladed turbine with a radius of 1 m is 7.5 m/s when the resistive torque is 1 Nm. This value over-estimates the actual cut-in speed by a factor of two according to the conclusion of Wood [31], which means the actual cut-in speed is nearly 4 m/s. Therefore, the designed wind speed ranging from 5.6 m/s to 8.5 m/s is used to study the efficiency of the proposed device. The simulation results are depicted in Fig. 7.

The results indicate that, keeping the optimal tip-speed ratio, a wind turbine with a radius of 1 m can extract the maximum mechanical power ranging from 152 W to 553 W when the wind speed varies from 5.6 m/s to 8.5 m/s, and the its crossponding angular velocity changes from 39 rad/s to 60 rad/s. Comparing the RMS of electric power in Fig. 6 with mechanical power in Fig. 7, we find that for the same angular velocity, the extracted wind power of the turbine is always higher than the RMS of the harvested electric power. For example, the wind turbine achieves a power of 308 W when the designed wind speed and angular velocity are 7.2 m/s and 50 rad/s, respectively. However, the RMS of the electric power is only 150 W when $\omega = 50$ rad/s, which is nearly half of the power extracted by the wind turbine. In addition, this gap becomes larger with an increase in the angular volecity. This finding means the efficiency of the proposed device at large angular velocity is lower than that at small values. The main reason for the low efficiency is that the resistive torque in Fig. 6 is only 1 Nm, and the low resistive torque leads to a small force applied to the piezoelectric bar. Mechanical and electric damping existed in the piezoelectricity-lever also makes the present harvester less effective at large angular velocity. Therefore, in the real practice, wind turbine with a larger radius is recommended in order to get a larger starting torque. Besides, a gearbox used to amplify the angular velocity can be adopted for generating a high electric power.

The effect of the ratio moment arms of the lever on the RMS of the electric power generated by the piezoelectric harvester can be clearly seen in Eqs. (11) and (12). Since the applied force is proportional to the ratio moment arms of the lever, a larger ratio of the moment arms of the lever will lead to a higher power generated by the piezoelectric bar. Fig. 8 gives the displacement of the equivalent mass m_e when $n = 20$. Wherein, the angular velocity, the stiffness of the spring, and the amplitude are 50 rad/s, 40,000 N/m, and 0.005 m, respectively. Since the maximal displacement in Fig. 8 is only 0.00094 m, it is reasonable to use a large ratio n in the real design which will not break the lever either.

Fig. 9 illustrates the effect of the width and length of the piezoelectric bar on the RMS of electric power. The angular velocity, the stiffness of the spring, the amplitude, and the ratio moment arms are set to be 50 rad/s, 40,000 N/m, 0.005 m, and 20, respectively. It can be found that the RMS nonlinearly decreases with an increase in the width and length of the piezoelectric bar. The RMS decreases from 150 W to74 W when the width and length of the piezoelectric bar change from 0.015 m to 0.025 m. The findings show that an increase in the width and length of the piezoelectric bar will lead to a rise in the electric capacity of c_a, and in turn a decrease in the electric voltage.

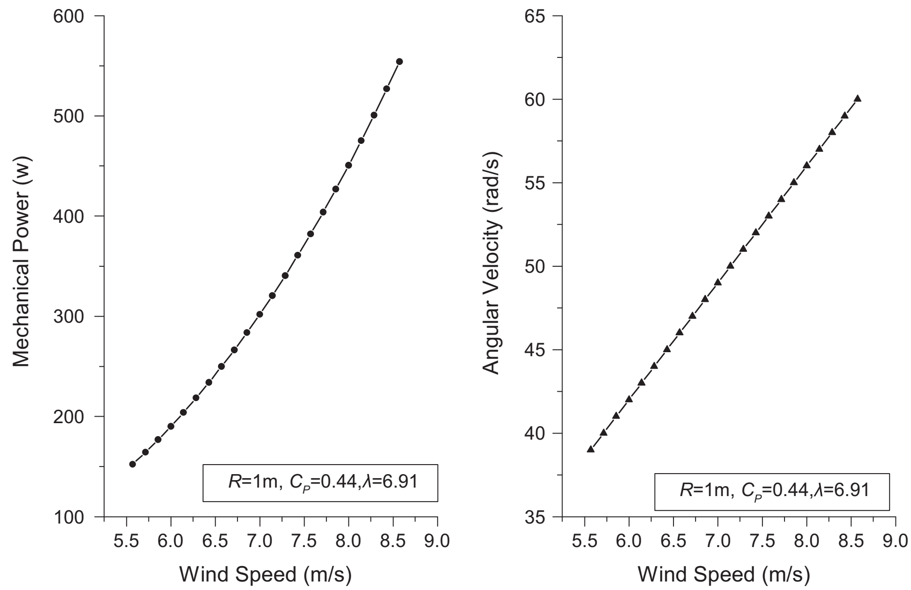

Fig. 7. The mechanical power and angular velocity versus wind speed.

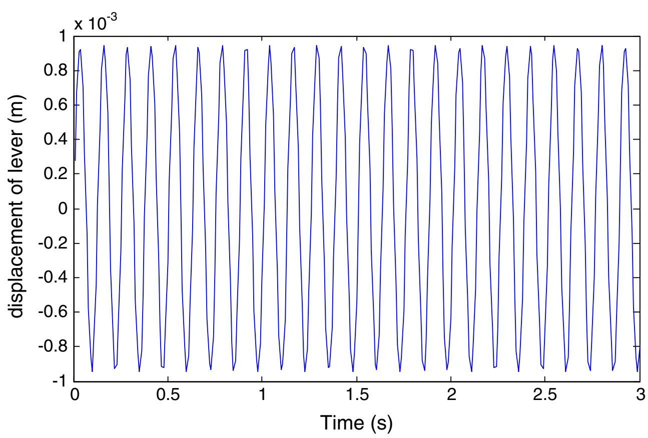

Fig. 8. Displacement of the equivalent mass m_e, $\omega = 50$ rad/s.

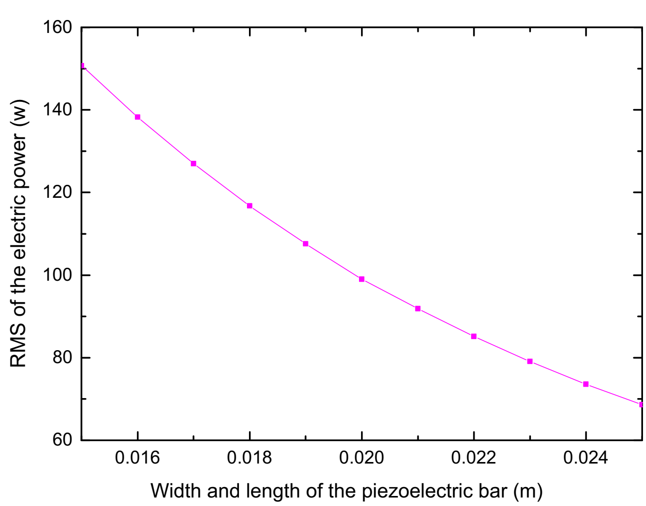

Fig. 9. RMS of the electric power versus width and length of the piezoelectric bar.

4. Conclusion

In this research, a practical piezoelectric wind turbine based on an engineering structure device is developed to harvest energy from wind. The Scotch yoke mechanism is adopted which is driven by rotating blades subjected to a force generated by wind. Hence, the rotational motion is converted into the linear motion of a slotted rod which is connected with two levers by springs. On the other side of the levers, there are two piezoelectric bars. The piezoelectric harvester transfers and amplifies the collected mechanical energy to electrical power. A mathematic model is developed to calculate the RMS of the generated electric power. The results show that, for a constant resistive torque, the RMS increases with an increase in the stiffness of the springs, angular velocity of the wind turbine, and the ratio of moment arms of the lever. Some experiential and theoretical formula of wind turbine are adopted to study the efficiency of the proposed device. The simulation results show that a power up to 150 W can be harvested for a piezoelectric wind turbine with a radius of blades of 1 m at the wind speed of 7.2 m/s, when the designed angular velocity is 50 rad/s. Based on the findings, it is possible to harvest a higher power by increasing the number and the radius of wind turbine rotor blades.

References

[1] Herbert GJ, Iniyan S, Sreevalsan E, Rajapandian S. A review of wind energy technologies. Renew Sustain Energy Rev 2007;11(6):1117–45.

[2] Verkinderen E, Imam B. A simplified dynamic model for mast design of H-Darrieus vertical axis wind turbines (VAWTs). Eng Struct 2015;100:564–76.

[3] Santangelo F, Failla G, Santini A, Arena F. Time-domain uncoupled analyses for seismic assessment of land-based wind turbines. Eng Struct 2016;123:275–99.

[4] Akwa JV, Vielmo HA, Petry AP. A review on the performance of Savonius wind turbines. Renew Sustain Energy Rev 2012;16(5):3054–64.

[5] Clausen P, Wood DH. Recent advances in small wind turbine technology. Wind Eng 2000;24(3):189–201.

[6] Burton T, Sharpe D, Jenkins N, Bossanyi E. Wind energy handbook. John Wiley and Sons; 2001.

[7] Priya S. Advances in energy harvesting using low profile piezoelectric transducers. J Electroceram 2007;19(1):167–84.

[8] Cook-Chennault KA, Thambi N, Sastry AM. Powering MEMS portable devices—a review of non-regenerative and regenerative power supply systems with special emphasis on piezoelectric energy harvesting systems. Smart Mater Struct 2008;17(4):043001.

[9] Priya S, Chen CT, Fye D, Zahnd J. Piezoelectric windmill: a novel solution to remote sensing. Jpn J Appl Phys 2004;44(1L):L104.

[10] Priya S. Modeling of electric energy harvesting using piezoelectric windmill. Appl Phys Lett 2005;87(18):184101.
[11] Myers R, Vickers M, Kim H, Priya S. Small scale windmill. Appl Phys Lett 2007;90(5):054106.
[12] Sirohi J, Mahadik R. Harvesting wind energy using a galloping piezoelectric beam. J Vib Acoust 2012;134(1):011009.
[13] Rezaei-Hosseinabadi N, Tabesh A, Dehghani R, Aghili A. An efficient piezoelectric windmill topology for energy harvesting from low-speed air flows. IEEE Trans Industr Electron 2015;62(6):3576–83.
[14] Kishore RA, Vučković D, Priya S. Ultra-low wind speed piezoelectric windmill. Ferroelectrics 2014;460(1):98–107.
[15] Wu N, Wang Q, Xie X. Wind energy harvesting with a piezoelectric harvester. Smart Mater Struct 2013;22(9):095023.
[16] Schoeftner J, Buchberger G. A contribution on the optimal design of a vibrating cantilever in a power harvesting application–Optimization of piezoelectric layer distributions in combination with advanced harvesting circuits. Eng Struct 2013;53:92–101.
[17] Luo Q, Tong L. Design and testing for shape control of piezoelectric structures using topology optimization. Eng Struct 2015;97:90–104.
[18] Song G, Sethi V, Li H-N. Vibration control of civil structures using piezoceramic smart materials: a review. Eng Struct 2006;28:1513–24.
[19] Xie XD, Wang Q, Wang SJ. Energy harvesting from high-rise buildings by a piezoelectric harvester device. Energy 2015;93:1345–52.
[20] Xie XD, Wang Q. Energy harvesting from a vehicle suspension system. Energy 2015;86:385–92.
[21] Wu N, Wang Q, Xie X. Ocean wave energy harvesting with a piezoelectric coupled buoy structure. Appl Ocean Res 2015;50:110–8.
[22] Xie XD, Wang Q. Design of a piezoelectric harvester fixed under the roof of a high-rise building. Eng Struct 2016;117:1–9.
[23] Viet NV, Xie XD, Liew KM, Banthia N, Wang Q. Energy harvesting from ocean waves by a floating energy harvester. Energy 2016;112:1219–26.
[24] https://en.wikipedia.org/wiki/Scotch_yoke#cite_note-1.
[25] Olutunde Oyadiji S, Qi S, Roger S. Development of multiple cantilevered piezo fibre composite beams vibration energy harvester for wireless sensor. In: Proceedings of the 4th world congress on engineering asset management, vol. 9; 2009. p. 28e30 [Athens, Greece].
[26] Blevins RD, Plunkett R. Formulas for natural frequency and mode shape. J Appl Mech 1980;47:461.
[27] Woodhouse J. Linear damping models for structural vibration. J Sound Vib 1998;215(3):547–69.
[28] Mitcheson PD, Yeatman EM, Rao GK, Holmes AS, Green TC. Energy harvesting from human and machine motion for wireless electronic devices. Proc IEEE 2008;96(9):1457–86.
[29] Rao SS, Yap FF. Mechanical vibrations, vol. 4. New York: Addison-Wesley; 1995.
[30] Slootweg JG, De Haan SWH, Polinder H, Kling WL. General model for representing variable speed wind turbines in power system dynamics simulations. IEEE Trans Power Syst 2003;18(1):144–51.
[31] Wood DH. A blade element estimation of the cut-in wind speed of a small turbine. Wind Eng 2001;25(4):249–55.